IEEE Access
Multidisciplinary | Rapid Review | Open Access Journal

Received July 17, 2020, accepted July 24, 2020, date of publication August 7, 2020, date of current version August 20, 2020.

Digital Object Identifier 10.1109/ACCESS.2020.3015052

Ecological Cooperative Adaptive Cruise Control for a Heterogeneous Platoon of Heavy-Duty Vehicles With Time Delays

CHUNJIE ZHAI[1], (Member, IEEE), XIYAN CHEN[1], CHENGGANG YAN[1], YONGGUI LIU[2], (Member, IEEE), AND HUAJUN LI[1]

[1]School of Automation, Hangzhou Dianzi University, Hangzhou 310018, China
[2]Key Laboratory of Autonomous Systems and Network Control, School of Automation Science and Engineering, Ministry of Education, South China University of Technology, Guangzhou 510641, China

Corresponding author: Chunjie Zhai (chunjiezhai2@gmail.com)

This work was supported in part by the National Natural Science Foundation of China under Grant 61931008, Grant 61671196, Grant 51906053, and Grant 61973128; and in part by the National Program on Key Basic Research Project under Grant 2017YFC0820605.

ABSTRACT To deal with energy crisis and environmental issues, higher fuel economy standards and more stringent limitations on greenhouse gas emissions for ground vehicles have been made. Ecological cooperative adaptive cruise control (Eco-CACC) has been considered as an effective solution to decrease the fuel consumption and greenhouse gas emissions of a platoon of vehicles, and this article proposes an Eco-CACC strategy for a heterogeneous platoon of heavy-duty vehicles with time delays. The proposed Eco-CACC strategy consists of distributed control protocols for the following vehicles and a new model predictive controller for the leading one. Firstly, after the distributed control protocols are designed based on the neighboring vehicle information, the sufficient conditions that guarantee the internal stability and string stability are derived, and the upper bound of the time delays under controller parameters is also obtained. Secondly, assuming the vehicle platoon as a rigid body with followers staying at desired positions, the new model predictive controller is designed in order to further improve the overall fuel economy of vehicle platoon. Simulations are conducted to validate the sufficient conditions of internal stability and string stability, and to explore the fuel saving performance of the proposed control strategy. The simulation results demonstrate that, compared with the benchmark, the proposed Eco-CACC strategy can significantly improve the fuel economy of heterogeneous platoon.

INDEX TERMS Cooperative control, heterogeneous platoon, string stability, model predictive control, fuel economy.

I. INTRODUCTION

The past decade has witnessed rapid increase of logistics industry and soaring of the number of automobiles in China [1]. Although the steadily growing logistics industry is boosting the economy and facilitating our daily life greatly, the transport system is facing greater challenges year by year, such as traffic congestion, traffic accidents and environmental pollution [2]. In order to solve such problems, increasing effort and massive energy have been devoted to the study of ecological cooperative adaptive cruise control (Eco-CACC) in recent years [3], [4].

The associate editor coordinating the review of this manuscript and approving it for publication was Emre Koyuncu.

The Eco-CACC is actually the combination of the platooning technology and the eco-driving technology [5], and it has the advantages of both the platooning technology and the eco-driving one. On the one hand, the Eco-CACC can organize a group of vehicles into a platoon, which can not only alleviate traffic congestion and enhance vehicle safety, but also improve fuel economy and reduce vehicle exhaust emissions thanks to the reduced aerodynamic drag [6], [7], on the other hand, without changing vehicular structure, the Eco-CACC can further decrease fuel consumption by making vehicles operate in a fuel-efficient way [8].

The existing Eco-CACC strategies can be divided into two categories, i.e., the intersection-based strategies and the highway-based ones. In the former, the traffic phase

This work is licensed under a Creative Commons Attribution 4.0 License. For more information, see https://creativecommons.org/licenses/by/4.0/

signal information is usually used, and the aerodynamic drag acting on vehicles can be ignored because the vehicles usually travel at low speeds. As far as we know, only a few intersection-based Eco-CACC strategies are achieved. A decentralized cooperative adaptive cruise control algorithm for vehicles in the vicinity of intersections was presented in [9] to maximize the intersection throughput by reorganizing the vehicle platoons, with fuel saving, velocity limitation, heterogeneous dynamics of vehicles and passenger comfort being taken into consideration. Using the signal phase and timing information, HomChaudhuri *et al.* proposed a fast model predictive control-based fuel-efficient control strategy for a group of connected vehicles in urban road conditions [10]. To minimize the delays over the entire trajectories for a platoon of autonomous vehicles, a green light optimal speed advisory system was put forward in [11] to reduce waiting delays and fuel consumption. He and Wu proposed an acceleration-based eco-driving advisory strategy for a mixed platoon of electric vehicles and gasoline vehicles in order to improve fuel economy [12].

Since vehicles on highways usually travel at high speeds, the aerodynamic drag is usually large, especially for the heavy-duty vehicles. Different from the intersection-based Eco-CACC strategies, by setting small inter-vehicle distances, the highway-based ones can further improve the overall fuel economy of vehicle platoon as the aerodynamic drag can be largely reduced [13]. To minimize the overall fuel consumption of a homogeneous platoon of automated vehicles, Li *et al.* presented the distributed servo loop controller based on dual-pulse-and-glide operation for each vehicle [13]. Even though the proposed control strategy in [13] can significantly decrease fuel consumption, the pulse-and-glide operation will reduce the comfort of passengers. To safely and fuel-efficiently coordinate a platoon of heavy-duty vehicles with continuous gear ratios, Turri *et al.* designed a two-layer control architecture [14], which is less practical because the dynamic programming used in the upper layer has the ''Curse of Dimensionality'' and cannot handle unexpected traffic disturbances. Guo *et al.* presented a two-layered hierarchical framework for truck platoon coordination: a speed planning layer for en route speed profile calculation and a control layer for vehicle speed tracking [1]. However, the aerodynamic drag acting on all vehicles and the different slopes of different vehicle positions are not considered when the platoon speed is planned, which might affect the overall fuel efficiency of vehicle platoon. To achieve vehicle safety, passenger comfort, formation control and fuel economy, a switched control strategy for heterogeneous following vehicles with state constraints was proposed in our previous published paper [15], in which the motion trajectory of the leading vehicle is not optimized. Hereafter, considering the influence of continuous variable transmission (CVT) on fuel consumption, we presented an ecological cooperative look-ahead control strategy for automated vehicles travelling on freeways with varying slopes in [5], where the motion trajectories of the following vehicles and the leading one are optimized based on model predictive control (MPC) in a distributed way. More highway-based Eco-CACC strategies can be found in [16]–[20].

In the vehicle platoon control, internal stability [21], [22] and string stability [23], [24] are two important performance indexes. Besides, the vehicle platoon control system is actually a networked control system with communication delays, sensor detection delay, actuator delay, braking delay, etc. These time delays need to be considered when designing the highway-based Eco-CACC strategies because they are critical factors when analyzing controller performance from traffic safety perspective [25]. In the existing highway-based Eco-CACC strategies, only the one in [18] can achieve both internal stability and string stability of vehicle platoon while considering the actuator delay. However, the upper bound of the actuator delay under the given controller parameters is not given in [18], and the control input of the leading vehicle is obtained by minimizing the leader's cost instead of the platoon's, which affects the further improvement of the platoon's fuel economy.

This article aims to propose an Eco-CACC strategy for a heterogeneous platoon of heavy-duty vehicles with time delays travelling on a highway with varying slopes, which consists of distributed control protocols for the following vehicles and model predictive controller for the leading one. Compared with the existing works, the main contributions of this article are as follows: (1) to ensure the internal stability and string stability of vehicle platoon under predecessor-leader following (PLF) communication topology, after the distributed control protocols are designed based on the neighboring vehicle information, the sufficient conditions that guarantee internal stability and string stability are derived, and the upper bound of the time delays under controller parameters is also obtained; (2) to improve the overall fuel economy of vehicle platoon, assuming the vehicle platoon as a rigid body with followers staying at desired positions, the new model predictive controller of the leading vehicle is designed by minimizing the total cost of vehicle platoon, in which the aerodynamic drag acting on all vehicles and the different slopes of different vehicle positions are considered. Furthermore, to explore the control performance of the proposed Eco-CACC strategy, extensive simulations have been carried out.

The remainder of this article is organized as follows: Section II presents the longitudinal dynamics model of vehicle platoon, the fuel consumption model and the control objectives of vehicle platoon, followed by the design and stability analysis of distributed control protocols in Section III. In Section IV, the new model predictive controller for the leader is presented. In Section V, the simulation results are discussed, followed by the conclusion of this article.

II. MODELING AND CONTROL OBJECTIVES

This article considers a heterogeneous platoon of heavy-duty vehicles under PLF communication topology running on a highway with varying slopes. And the platoon consists of

one lead vehicle (indexed by 0) and N followers (indexed from 1 to N). This section will present the longitudinal dynamics model of vehicle platoon, the fuel consumption model, and the control objectives of vehicle platoon.

A. LONGITUDINAL DYNAMICS MODEL OF VEHICLE PLATOON

In the existing studies on vehicle platoon control, the exact linearization is utilized to derive an exact linear model for the upper level longitudinal dynamics of a vehicle. To describe the upper level longitudinal dynamics, some researchers employed second-order differential models [3], [15], [16], while others adopted third-order differential models [5], [26], [27]. In this article, a second-order differential model will be applied to describe the upper level longitudinal dynamics of vehicles in the platoon.

According to [14], the upper level longitudinal dynamics model of heavy-duty vehicle platoon at time t can be given as

$$\begin{cases} \dot{p}_i(t) = v_i(t) \\ \dot{v}_i(t) = u_i(t), \end{cases} \tag{1}$$

where p_i, v_i and u_i are the position, velocity and control input of vehicle i, respectively.

According to the Newton's second law, the relationship among the control input u_i, the desired engine output power $P_{i,e}$, the braking force $B_i(t)$ and the integrated resistance force $F_{i,r}$ can be given as

$$m_i \cdot u_i(t) = \frac{\eta_{i,t} P_{i,e}(t)}{v_i(t)} - B_i(t) - F_{i,r}(t), \tag{2}$$

where m_i is the mass of vehicle i, and the integrated resistance force can be described as

$$F_{i,r}(t) = m_i g(\mu_i cos(\theta(p_i(t))) + sin(\theta(p_i(t)))) + \frac{C_d(d_i(t))\rho A_{i,v} v_i^2(t)}{2}. \tag{3}$$

In (3), $C_d(d_i(t))$, $A_{i,v}$, μ_i and $\theta(p_i(t))$ are the drag coefficient related to vehicle spacing $d_i(t)$, frontal area, rolling coefficient and road slope related to position, respectively; ρ and g are the air density and gravitational acceleration, respectively. And the spacing $d_i(t)$ can be calculated through

$$d_i(t) = p_{i-1}(t) - p_i(t) - L_i, \tag{4}$$

where L_i is the length of vehicle i.

Furthermore, according to [14], the drag coefficient C_d can be given as

$$C_d(d_i(t)) = \begin{cases} C_{i,d}, & \text{if } i = 0 \\ C_{i,d}(1 - \dfrac{c_1}{c_2 + d_i(t)}), & \text{else} \end{cases} \tag{5}$$

where $C_{i,d}$ is the nominal drag coefficient of vehicle i, and the parameters c_1 and c_2 are obtained by regressing the experimental data presented in [28].

B. FUEL CONSUMPTION MODEL

According to [1], the fuel consumption rate of a vehicle is influenced by many factors, e.g., air resistance, mass, engine power, tire size/pressure, road conditions and others. For simplicity, same as [1], [14], [17], the CVT-type powertrain is also considered in this article, and the gear ratio management system is assumed to select the gear ratio to ensure that the engine works along the optimal engine operating line. Then, the fuel consumption rate depends the engine output power only, and can be estimated using the fuel consumption model in [29].

According to [29], the fuel consumption rate $FC_i(t)$ of vehicle i can be given as

$$FC_i(t) = \begin{cases} \gamma_0 + \gamma_1 P_{i,e}(t) + \gamma_2 (P_{i,e}(t))^2, & \text{if } P_{i,e}(t) \geq 0 \\ \gamma_0, & \text{else} \end{cases} \tag{6}$$

where γ_0, γ_1 and γ_2 are the coefficients of fuel consumption model.

C. CONTROL OBJECTIVES

In general, two policies can be employed for spacing control of platoons, i.e., the constant spacing (CS) policy [25], [30], [31] and the constant time headway (CTH) one [32]–[34]. In the CS policy, the desired spacing between consecutive vehicles is constant, while the desired spacing is a function of velocity in the CTH policy.

In this article, to improve road capacity, the CS policy will be used to regulate the inter-vehicle distance, which needs information of the leader to ensure string stability of vehicle platoon [35], [36]. Let p_i^* and v_i^* be the desired position and velocity of vehicle i, respectively, which are defined as

$$\begin{cases} p_i^*(t) = p_0(t) - \sum_{m=1}^{i} (L_i + d), & \text{if } i \geq 1 \\ v_i^*(t) = v_0(t), & \text{else} \end{cases} \tag{7}$$

where d indicates the desired spacing between adjacent vehicles.

Then, the position error $\tilde{p}_i(t)$ and velocity error $\tilde{v}_i(t)$ of following vehicle i can be defined as

$$\begin{cases} \tilde{p}_i(t) = p_i(t) - p_i^*(t), \\ \tilde{v}_i(t) = v_i(t) - v_i^*(t). \end{cases} \tag{8}$$

i) Internal stability

When the acceleration of the lead vehicle is zero, all followers under the distributed control protocols will stay at the desired positions and reach the same velocity as the leader over time, i.e.,

$$\begin{cases} \lim_{t\to\infty} p_i(t) = p_i^*(t) \\ \lim_{t\to\infty} v_i(t) = v_i^*(t) \end{cases} \tag{9}$$

for $i = 1, 2, \cdots, N$.

ii) String stability

The spacing error $e_i(t)$ of vehicle i can be given as

$$e_i(t) = d_i(t) - d. \tag{10}$$

Let $E_i(s)$ be the Laplace transform of the position error $e_i(t)$, same as [1], the string stability condition can be given as

$$\left\| \frac{E_i(j\omega)}{E_{i-1}(j\omega)} \right\| \leq 1, \quad \forall\omega. \tag{11}$$

where Laplace operator s is replaced by $j\omega$.

iii) Fuel economy

The overall fuel consumption of vehicle platoon should be as small as possible when the platoon travels on a highway with varying slopes for a certain period of time. The total fuel consumption from time t to $t+T$ can be obtained as $\sum_{i=0}^{N}\int_t^{t+T} FC_i(P_{i,e}(\tau))d\tau$. The vehicles in the platoon should adjust their throttles, brakes and gear ratios during time $t \sim t+T$ to minimize $\sum_{i=0}^{N}\int_t^{t+T} FC_i(P_{i,e}(\tau))d\tau$.

III. DISTRIBUTED CONTROL PROTOCOLS

This section will design the distributed control protocols for the following vehicles in the platoon under PLF communication topology, and the sufficient conditions that guarantee the internal stability and string stability of vehicle platoon will be derived. Furthermore, the upper bound of the time delays under controller parameters is also obtained.

Firstly, for the vehicle platoon with time delays, the distributed control protocols are designed as

$$\begin{aligned} u_i(t) = {} & \ddot{p}_i^*(t) - \alpha[p_i(t-\tau_i) - p_i^*(t-\tau_i) + v_i(t-\tau_i) \\ & - v_i^*(t-\tau_i)] - \beta[p_i(t-\tau_i) - p_{i-1}(t-\tau_i) + L_i + d \\ & + v_i(t-\tau_i) - v_{i-1}(t-\tau_i)], \end{aligned} \tag{12}$$

where τ_i denotes the input delay, which includes the measuring delay of sensors, the communication delay, and the breaking/throttle delay, etc. In addition, $\ddot{p}_i^*(t)$ denoting the acceleration of the lead vehicle can be obtained by follower i without input delay because the leader can tell followers about its intended acceleration sequence in the future, which will be detailed in Section IV.

Usually, the input delays are stochastic and various. In order to derive the upper bound of input delays, these input delays are assumed to be identical and constant but unknown τ. In reality, a buffer memory may be employed to ensure that all the stochastic time-delays are further delayed intentionally (if required) to some constant τ, which is similar to [25].

Then, the control law in (12) can be rewritten as

$$\begin{aligned} u_i(t) = {} & \ddot{p}_i^*(t) - \alpha[p_i(t-\tau) - p_i^*(t-\tau) + v_i(t-\tau) \\ & - v_i^*(t-\tau)] - \beta[p_i(t-\tau) - p_{i-1}(t-\tau) + L_i + d \\ & + v_i(t-\tau) - v_{i-1}(t-\tau)]. \end{aligned} \tag{13}$$

A. INTERNAL STABILITY ANALYSIS

When the leader travels at a steady speed, the distributed control protocols in (13) can be rewritten as

$$\begin{aligned} u_i(t) = {} & -\alpha[p_i(t-\tau) - p_i^*(t-\tau) + v_i(t-\tau) \\ & - v_i^*(t-\tau)] - \beta[p_i(t-\tau) - p_{i-1}(t-\tau) + L_i + d \\ & + v_i(t-\tau) - v_{i-1}(t-\tau)], \end{aligned} \tag{14}$$

Let $p(t) \triangleq [p_1(t), \cdots, p_N(t)]^T$, $v(t) \triangleq [v_1(t), \cdots, v_N(t)]^T$, $p^*(t) \triangleq [p_1^*(t), \cdots, p_N^*(t)]^T$, $v^*(t) \triangleq [v_1^*(t), \cdots, v_N^*(t)]^T$, and define $\tilde{p}(t) \triangleq p(t) - p^*(t)$, $\tilde{v}(t) \triangleq v(t) - v^*(t)$, and $x(t) = [\tilde{p}(t)^T, \tilde{v}(t)^T]^T$, then the second-order dynamics of the platoon can be given as

$$\dot{x}(t) = \mathbb{L}_1 x(t) + \mathbb{L}_2 x(t-\tau), \tag{15}$$

where

$$\mathbb{L}_1 = \begin{bmatrix} 0_{N\times N} & I_N \\ 0_{N\times N} & 0_{N\times N} \end{bmatrix} \tag{16}$$

and

$$\mathbb{L}_2 = \begin{bmatrix} 0_{N\times N} & 0_{N\times N} \\ -(\alpha I_N + \beta L) & -(\alpha I_N + \beta L) \end{bmatrix}. \tag{17}$$

Furthermore, L in (17) denoting the Laplace matrix under the PLF topology can be described as

$$L = \begin{bmatrix} 0 & & & \\ -1 & 1 & & \\ & \ddots & \ddots & \\ & & -1 & 1 \end{bmatrix}_{N\times N}. \tag{18}$$

Let $X(s)$ be the Laplace transform of $x(t)$ under the given initial condition x(0), then one can have

$$X(s) = (sI_{2N} - \mathbb{L}_1 - \mathbb{L}_2 e^{-\tau s})^{-1} x(0). \tag{19}$$

Theorem 1: Consider the second-order dynamics system (15) deduced by each vehicle (1) and the control protocols (14), the internal stability of vehicle platoon can be guaranteed if the control parameters meet

$$\begin{cases} \alpha > 0 \\ \beta > 0 \\ \tau < \tau_s, \end{cases} \tag{20}$$

where

$$\tau_s = \frac{\arctan\left(\sqrt{\frac{(\alpha+\beta)^2+(\alpha+\beta)\sqrt{(\alpha+\beta)^2+4}}{2}}\right)}{\sqrt{\frac{(\alpha+\beta)^2+(\alpha+\beta)\sqrt{(\alpha+\beta)^2+4}}{2}}}. \tag{21}$$

Proof: The eigenvalues of $sI_{2n} - \mathbb{L}_1 - \mathbb{L}_2 e^{-\tau s}$ determine the internal stability of the system in (15). By solving $\det(sI_{2n} - \mathbb{L}_1 - \mathbb{L}_2 e^{-\tau s}) = 0$, one can have

$$\det(sI_{2N} - \mathbb{L}_1 - \mathbb{L}_2 e^{-\tau s}) = \prod_{i=1}^{N}[s^2 + (\alpha + \beta\lambda_i)(s+1)e^{-\tau s}] = 0, \tag{22}$$

where λ_i is the ith eigenvalue of L. Since the PLF topology is used in this article, $\lambda_i = 0$ or 1.

Further, one can have

$$s^2 + \alpha(s+1)e^{-\tau s} = 0 \tag{23}$$

and

$$s^2 + (\alpha+\beta)(s+1)e^{-\tau s} = 0. \tag{24}$$

To ensure the internal stability of the system, the real parts of characteristic roots in characteristic equations (23) and (24) must be negative. Considering the time delay, the Nyquist stability criterion will be adopted to obtain the sufficient condition of internal stability.

Firstly, the characteristic equation (23) has the same characteristic roots as a unit negative feedback system with the open loop transfer function $G_0(s)$ being

$$G_0(s) = \frac{\alpha(s+1)e^{-\tau s}}{s^2}. \tag{25}$$

Let $s = j\omega$, then the frequency response corresponding to the open-loop transfer function $G_0(s)$ can be given as

$$G_0(j\omega) = \frac{\alpha(j\omega+1)e^{-j\tau\omega}}{-\omega^2}. \tag{26}$$

The amplitude function of $G_0(j\omega)$ is

$$A_0(\omega) = \frac{\alpha\sqrt{\omega^2+1}}{\omega^2}. \tag{27}$$

The phase angle function of $G_0(j\omega)$ is

$$\phi_0(\omega) = \arctan(\omega) - \tau\omega - \pi. \tag{28}$$

The first derivatives of the amplitude function $A_0(\omega)$ and the phase angle function $\phi_0(\omega)$ are

$$\begin{cases} \dot{A}_0(\omega) = -\alpha\omega\dfrac{\omega^2+2}{\omega^4\sqrt{\omega^2+1}}, \\ \dot{\phi}_0(\omega) = \dfrac{1}{1+\omega^2} - \tau. \end{cases} \tag{29}$$

When ω goes from 0^+ to $+\infty$, it is obvious that the amplitude function $A_0(\omega)$ monotonically decreases, and the phase angle function $\phi_0(\omega)$ increases monotonically first and then decreases monotonically due to the fact that τ is much smaller than 1 s in reality.

It is obvious that there is only one positive solution of $\phi_0(\omega) = -\pi$. Assuming ω_c is the solution of $\phi_0(\omega) = -\pi$, it is easy to have

$$\phi_0(\omega) > -\pi, \quad 0 < \omega < \omega_c. \tag{30}$$

Assuming ω_g is the solution of $A_0(\omega) = 1$, then one can achieve $\omega_g = \sqrt{\frac{\alpha^2+\alpha\sqrt{\alpha^2+4}}{2}}$. According to the Nyquist stability criterion, the unit negative feedback system is stable if $\phi_0(\omega_g) > -\pi$.

Then, the upper bound of input delay that the real parts of characteristic roots in characteristic equations (23) are negative is

$$\tau < \frac{\arctan(\omega_g)}{\omega_g} = \frac{\arctan(\sqrt{\frac{\alpha^2+\alpha\sqrt{\alpha^2+4}}{2}})}{\sqrt{\frac{\alpha^2+\alpha\sqrt{\alpha^2+4}}{2}}} = \tau_m. \tag{31}$$

Applying the same method to the characteristic equation (24), the upper bound of input delay that the real parts of characteristic roots in characteristic equations (24) are negative is

$$\tau < \frac{\arctan(\sqrt{\frac{(\alpha+\beta)^2+(\alpha+\beta)\sqrt{(\alpha+\beta)^2+4}}{2}})}{\sqrt{\frac{(\alpha+\beta)^2+(\alpha+\beta)\sqrt{(\alpha+\beta)^2+4}}{2}}} = \tau_s. \tag{32}$$

Let $f(\omega) = \frac{\arctan(\omega)}{\omega}$, and it is easy to derive that $f(\omega)$ monotonically decreases when ω goes from 0^+ to $+\infty$. Since $0 < \sqrt{\frac{\alpha^2+\alpha\sqrt{\alpha^2+4}}{2}} < \sqrt{\frac{(\alpha+\beta)^2+(\alpha+\beta)\sqrt{(\alpha+\beta)^2+4}}{2}}$, to ensure the internal stability of the system in (15), the sufficient conditions can be given as

$$\begin{cases} \alpha > 0 \\ \beta > 0 \\ \tau < \tau_s. \end{cases} \tag{33}$$

Then, the proof of **Theorem 1** is finished.

B. STRING STABILITY ANALYSIS

Combining (1), (7) and (13), one can have

$$\begin{aligned} \ddot{\tilde{p}}_i(t) = &-(\alpha+\beta)\dot{\tilde{p}}_i(t-\tau) - (\alpha+\beta)\tilde{p}_i(t-\tau) \\ &+ \beta(\dot{\tilde{p}}_{i-1}(t-\tau) + \tilde{p}_{i-1}(t-\tau)). \end{aligned} \tag{34}$$

Theorem 2: Consider the second-order dynamics system (34) deduced by each vehicle (1) and the control protocols (13), the internal stability and string stability of vehicle platoon can be guaranteed if the control parameters meet

$$\begin{cases} 0 < \alpha < 4, \\ \beta > 0, & \text{if } \alpha = 1 \\ \beta_{min} < \beta \le \beta_{max}, & \text{if } 0 < \alpha < 1 \text{ or } 1 < \alpha < 4 \\ \tau < \min\{\tau_s, \tau_{ss}\}, \end{cases} \tag{35}$$

where

$$\begin{cases} \beta_{min} = \max\{\dfrac{\alpha^2(3-\alpha) - 2\alpha^{\frac{3}{2}}}{2(\alpha-1)^2}, 0\} \\ \beta_{max} = \dfrac{\alpha^2(3-\alpha) + 2\alpha^{\frac{3}{2}}}{2(\alpha-1)^2} \\ \tau_{ss} = \dfrac{1}{2(\alpha+\beta)}. \end{cases} \tag{36}$$

Proof: Taking Laplace transform for (34) under the zero initial condition, it is easy to have

$$\begin{aligned} s^2\tilde{P}_i(s) = &-(\alpha+\beta)e^{-\tau s}(s+1)\tilde{P}_i(s) \\ &+ \beta(s+1)e^{-\tau s}\tilde{P}_{i-1}(s), \end{aligned} \tag{37}$$

where $\tilde{P}_i(s)$ and $\tilde{P}_{i-1}(s)$ are the Laplace transform of $\tilde{p}_i$ and $\tilde{p}_{i-1}$, respectively.

Reorganizing (37), one can further have

$$\frac{\tilde{P}_i(s)}{\tilde{P}_{i-1}(s)} = \frac{\beta(s+1)e^{-\tau s}}{s^2 + (\alpha+\beta)(s+1)e^{-\tau s}}. \tag{38}$$

Furthermore, according to (4) and (10), one can have

$$\begin{aligned} e_i(t) &= p_{i-1}(t) - p_i(t) - L_i - d \\ &= p_{i-1}(t) - p^*_{i-1}(t) + p^*_{i-1}(t) - L_i - d - p_i(t) \\ &= p_{i-1}(t) - p^*_{i-1}(t) + p^*_i(t) - p_i(t) \\ &= \tilde{p}_{i-1}(t) - \tilde{p}_i(t) \end{aligned} \tag{39}$$

Taking Laplace transform for (39) under the zero initial condition, it is easy to have

$$E_i(s) = \tilde{P}_{i-1}(s) - \tilde{P}_i(s). \tag{40}$$

Then, one has

$$\begin{aligned} \frac{E_{i+1}(s)}{E_i(s)} &= \frac{\tilde{P}_i(s) - \tilde{P}_{i+1}(s)}{\tilde{P}_{i-1}(s) - \tilde{P}_i(s)} = \frac{1 - \frac{\tilde{P}_{i+1}(s)}{\tilde{P}_i(s)}}{\frac{\tilde{P}_{i-1}(s)}{\tilde{P}_i(s)} - 1} \\ &= \frac{\beta(s+1)e^{-\tau s}}{s^2 + (\alpha+\beta)(s+1)e^{-\tau s}}. \end{aligned} \tag{41}$$

According to the string stability definition in (11), one has

$$\left\| \frac{\beta(j\omega+1)e^{-j\tau\omega}}{-\omega^2 + (\alpha+\beta)(j\omega+1)e^{-j\tau\omega}} \right\| \leq 1, \quad \forall\omega. \tag{42}$$

Since $e^{-j\tau\omega} = \cos(\tau\omega) - j\sin(\tau\omega)$, from (42), it is easy to have

$$\begin{aligned} &\omega^4 - 2(\alpha+\beta)\sin(\omega\tau)\omega^3 \\ &\quad + [\alpha(\alpha+2\beta) - 2(\alpha+\beta)\cos(\omega\tau)]\omega^2 \\ &\quad + \alpha(\alpha+2\beta) \geq 0 \end{aligned} \tag{43}$$

Using the fact that

$$\begin{aligned} \sin(\omega\tau) \leq \omega\tau &\Rightarrow -2(\alpha+\beta)\omega^3\sin(\omega\tau) \\ &\geq -2(\alpha+\beta)\tau\omega^4 \\ \cos(\omega\tau) \leq 1 &\Rightarrow -2(\alpha+\beta)\cos(\omega\tau) \\ &\geq -2(\alpha+\beta), \end{aligned} \tag{44}$$

then, one has

$$a_4\omega^4 + a_2\omega^2 + a_0 \geq 0, \tag{45}$$

where $a_4 = 1 - 2(\alpha+\beta)\tau$, $a_2 = \alpha(\alpha+2\beta) - 2(\alpha+\beta)$, and $a_0 = \alpha(\alpha+2\beta)$. The inequality in (45) always holds if $\Delta = a_2^2 - 4a_4a_0 \leq 0$ and $a_4 > 0$.

Then, one can derive

$$4(\alpha-1)^2\beta^2 + 4\alpha^2(\alpha-3)\beta + \alpha^3(\alpha-4) \leq 0, \tag{46}$$

and

$$\tau < \frac{1}{2(\alpha+\beta)} = \tau_{ss}. \tag{47}$$

One further derives that

$$\begin{cases} 0 < \alpha < 4 & \\ \beta > 0, & \text{if } \alpha = 1 \\ \beta_{min} < \beta \leq \beta_{max}, & \text{if } 0 < \alpha < 1 \text{ or } 1 < \alpha < 4 \end{cases} \tag{48}$$

where

$$\begin{cases} \beta_{min} = \max\{\dfrac{\alpha^2(3-\alpha) - 2\alpha^{\frac{3}{2}}}{2(\alpha-1)^2}, 0\} \\ \beta_{max} = \dfrac{\alpha^2(3-\alpha) + 2\alpha^{\frac{3}{2}}}{2(\alpha-1)^2}. \end{cases} \tag{49}$$

Combining (20), (47) and (48), the proof of **Theorem 2** is finished.

Remark 1: In the string stability analysis, the upper bound of the input delay is obtained under the given controller parameters α and β. It can be known from **Theorem 2** that the upper bound of the input delay is negatively correlated with $\alpha + \beta$. The larger $\alpha + \beta$, the smaller the upper bound of the input delay.

IV. MODEL PREDICTIVE CONTROL

This section aims to optimize the control input of the lead vehicle based on MPC in order to decrease the overall fuel consumption of vehicle platoon. To achieve that, firstly, the vehicle platoon is assumed to be a rigid body, in which all followers stay at the desired positions; secondly, the control input optimization problem of the lead vehicle (CIO-LV) is formulated based on MPC, in which passenger comfort requirements and physical limitations of vehicle platoon are considered; thirdly, an improved particle swarm optimization (PSO) algorithm is used to solve the formulated optimization problem quickly.

A. BAND-STOP FUNCTION

The band-stop function with compensating factors used in [5] will also be employed in the CIO-LV problem. The band-stop function is given as

$$BSF(z|\hat{\alpha}, \hat{\beta}, \hat{n}, z_l, z_u, c) = \left(\frac{e^{-\hat{\alpha}(z-z_l-c)} + e^{\hat{\alpha}(z-z_u+c)}}{\hat{\beta}}\right)^{\hat{n}}, \tag{50}$$

where $\hat{\alpha} > 0$, $\hat{\beta} \geq 1$ and $\hat{n} \in N^+$. z_l, $z_u \in \mathbb{R}^+$ are the lower and upper limits of the band $[z_l, z_u]$, respectively. In addition, c is the compensating factor.

In an optimization problem, in which the band-stop function $BSF(z|\hat{\alpha}, \hat{\beta}, \hat{n}, z_l, z_u, c)$ acts as a part of the cost function, z can be forced around, even in the band $[z_l, z_u]$ if the parameters $\hat{\alpha}$, $\hat{\beta}$, $\hat{n}$ and c are set properly.

B. CIO-LV BASED ON MPC

Let Δt be the discrete time interval, according to (1), considering the input delay, the discrete longitudinal dynamics model of the leading vehicle can be given as

$$\begin{cases} p_0(k+1) = p_0(k) + v_0(k) \cdot \Delta t \\ v_0(k+1) = v_0(k) + u_0(k-D) \cdot \Delta t, \end{cases} \tag{51}$$

where $D = \lceil \frac{\tau}{\Delta t} \rceil$.

Let $x_0 = [p_0, v_0]^T$, then (51) can be further expressed as

$$x_0(k+1) = A_0x_0(k) + B_0u_0(k-D), \tag{52}$$

where

$$\begin{cases} A_0 = \begin{bmatrix} 1 & \Delta t \\ 0 & 1 \end{bmatrix} \\ B_0 = \begin{bmatrix} 0 \\ \Delta t \end{bmatrix}. \end{cases} \tag{53}$$

Since all the followers are assumed to stay at the desired positions in the vehicle platoon, the position, velocity and control input of follower i can be given as

$$\begin{cases} p_i(k) = p_0(k) - \sum_{m=1}^{i}(L_m + d) \\ v_i(k) = v_0(k) \\ u_i(k) = u_0(k). \end{cases} \tag{54}$$

According to the distributed control protocols (12), the acceleration of the leading vehicle can be obtained by followers without delay, which can be ensured by telling followers about intended acceleration sequence of the leader in the future. Next, we will explain how this can be done.

Let N_p and N_c be the predictive horizon and the control horizon, respectively, and the MPC frameworks are given in FIGURE 1. As shown in FIGURE 1, the blue arrows represent the typical MPC framework, under which the N_c control variables can be obtained by solving the MPC-based optimization problem when the current control horizon ends. In this article, to inform followers of the intended accelerations of the leader in the future, the future N_c accelerations of the leader should be obtained before the current control horizon ends.

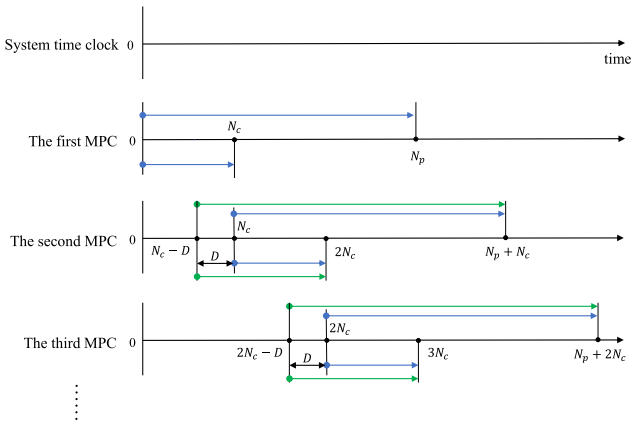

FIGURE 1. The MPC frameworks.

As shown in FIGURE 1, considering the time delay D, the N_c accelerations in the second MPC should be obtained at time $N_c - D$ so that followers can know the leader's accelerations in the time range $[N_c, 2N_c)$. It should be noted that the accelerations of the leader in the time range $[N_c - D, N_c)$ stay unchanged, and the predictive horizon is still $N_c \sim N_p + N_c$. Therefore, the new MPC framework represented by the green arrows in FIGURE 1 will be used to achieve the accelerations of the leader.

Let $\tilde{k} = k + 2D$, considering the input delay of the leader and the new MPC framework, before formulating the CIO-LV problem at time k, some predictive variables over the predictive horizon $\tilde{k} \sim \tilde{k} + N_p$ are defined as follows:

- $x_i(n+1|\tilde{k})$: the predictive state of vehicle i at time $\tilde{k}+n+1$;
- $p_i(n|\tilde{k})$: the predictive position of vehicle i at time $\tilde{k}+n$;
- $v_i(n|\tilde{k})$: the predictive velocity of vehicle i at time $\tilde{k}+n$;
- $u_i(n|\tilde{k})$: the predictive control input of vehicle i at time $\tilde{k}+n$;
- $P_{i,e}(n|\tilde{k})$: the predictive engine output power of vehicle i at time $\tilde{k}+n$;
- $FC_i(n|\tilde{k})$: the predictive fuel consumption rate of vehicle i at time $\tilde{k}+n$.

The cost function of vehicle i in the predictive horizon can be given as

$$\begin{aligned} f_i(\tilde{k}) &= w_1 \frac{1}{p_i(N_p|\tilde{k}) - p_i(0|\tilde{k})} + w_2 \sum_{n=0}^{N_p-1} FC_i(n|\tilde{k}) \cdot \Delta t \\ &\quad + w_3 \sum_{n=1}^{N_p} BSF(v_i(n|\tilde{k})|\hat{\alpha}, \hat{\beta}, \hat{n}, v_l, v_u, c) \\ &= w_1 \frac{1}{p_0(N_p|\tilde{k}) - p_0(0|\tilde{k})} + w_2 \sum_{n=0}^{N_p-1} FC_i(n|\tilde{k}) \cdot \Delta t \\ &\quad + w_3 \sum_{n=1}^{N_p} BSF(v_0(n|\tilde{k})|\hat{\alpha}, \hat{\beta}, \hat{n}, v_l, v_u, c), \end{aligned} \tag{55}$$

where w_1, w_2 and w_3 are the weight parameters while v_l and v_u are the lower and upper limits of the desired velocity band $[v_l, v_u]$ of vehicle platoon.

Further, the cost function of vehicle platoon in the predictive horizon can be obtained as

$$\begin{aligned} F(\tilde{k}) &= \sum_{i=0}^{N} f_i(\tilde{k}) \\ &= \frac{w_1(I+1)}{p_0(N_p|\tilde{k}) - p_0(0|\tilde{k})} + w_2 \sum_{i=0}^{I} \sum_{n=0}^{N_p-1} FC_i(n|\tilde{k}) \cdot \Delta t \\ &\quad + w_3 \sum_{i=0}^{I} \sum_{n=1}^{N_p} BSF(v_0(n|\tilde{k})|\hat{\alpha}, \hat{\beta}, \hat{n}, v_l, v_u, c). \end{aligned} \tag{56}$$

After the predictive variables and the cost function of vehicle platoon are given, the CIO-LV problem can be formulated as

$$u_0^*(:|\tilde{k}) = \arg\min_{u_0(:|\tilde{k})} F(\tilde{k}),$$

$$\text{subject to} \begin{cases} x_0(n+1|\tilde{k}) = A_0 x_0(n|\tilde{k}) + B_0 u_0(n|\tilde{k}) \\ p_i(n|\tilde{k}) = p_0(n|\tilde{k}) - \sum_{m=1}^{i}(L_m + d) \\ v_i(n|\tilde{k}) = v_0(n|\tilde{k}) \\ m_i \cdot u_0(n|\tilde{k}) = \dfrac{\eta_{i,t} P_{i,e}(n|\tilde{k})}{v_i(n|\tilde{k})} \\ -B_i(n|\tilde{k}) - F_{i,r}(n|\tilde{k}) \\ u_{0,min} \le u_0(n|\tilde{k}) \le u_{0,max} \\ i = 0, 1, 2, \cdots, N. \end{cases} \tag{57}$$

where $F_{i,r}(n|\tilde{k})$ and $FC_i(n|\tilde{k})$ can be calculated through

$$F_{i,r}(n|\tilde{k}) = m_i g(\mu_i cos(\theta(p_i(n|\tilde{k}))) + sin(\theta(p_i(n|\tilde{k})))) + \frac{C_d(d)\rho A_{i,v} v_i^2(n|\tilde{k})}{2} \tag{58}$$

and

$$FC_i(n|\tilde{k}) = \begin{cases} \gamma_0 + \gamma_1 P_{i,e}(n|\tilde{k}) \\ +\gamma_2 (P_{i,e}(n|\tilde{k}))^2, & \text{if } P_{i,e}(n|\tilde{k}) \ge 0 \\ \gamma_0, & \text{else.} \end{cases} \tag{59}$$

In the formulated CIO-LV problem, $u_0(:|\tilde{k}) = [u_0(0|\tilde{k}), u_0(1|\tilde{k}), \cdots, u_0(N_p - 1|\tilde{k})]$ denote the unknown predictive control variables to be optimized, and $u_0^*(:|\tilde{k})$ indicate the optimal predictive control variables that minimize the cost function $F(\tilde{k})$. Due to external disturbances and model uncertainties, the first N_c optimal control variables $[u_0^*(0|\tilde{k}), \cdots, u_0^*(N_c - 1|\tilde{k})]$ will be used as the control inputs in the time range $[\tilde{k}, \cdots, \tilde{k} + N_c)$.

Since the CIO-LV problem is a constrained nonlinear nonconvex optimization one, it is very challenging to quickly obtain the optimal solution. Possessed of several desired attributes, such as global search, parallel capabilities, easy implementing, reduced memory requirement and no calculations of the gradient, the improved PSO algorithm in [5] will be used to solve the CIO-LV problem.

V. SIMULATIONS

In this section, the performance of the proposed Eco-CACC strategy will be investigated comprehensively. According to [37], one leader and at least two following vehicles are needed to analyze the string stability of a vehicle platoon. Therefore, a heterogeneous platoon with one leader and five followers are considered in the simulation. Since the real highway can be regarded as a combination of road sections with different constant slopes, the simulated highway utilized in the simulation is given in FIGURE 2.

To show the effectiveness of the proposed Eco-CACC strategy on reducing the fuel consumption of vehicle platoon, the cruise control strategy with the space gap policy (CC-SG) in [14] will be used as the benchmark. In addition, for fair comparison, the reference speed for the CC-SG strategy is properly set so that Eco-CACC and CC-SG have the same average speed, and the proposed distributed control protocols with the same controller parameters are used to control the followers for Eco-CACC and CC-SG.

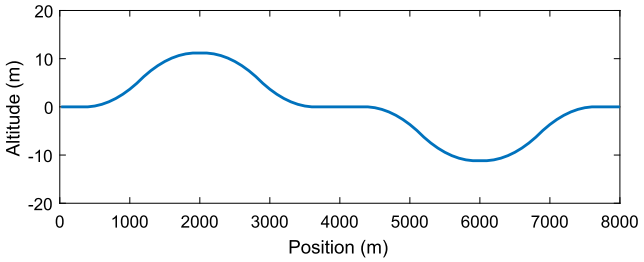

FIGURE 2. The simulated highway with varying slopes.

In the simulation, the parameters of vehicle dynamics model are given in TABLE 1, which are properly set according to [29]; the discrete time interval is set as $\Delta t = 0.1$ s; the predictive and control horizon lengths in the CIO-LV problem are set as $N_p = 20$ and $N_c = 4$; the lower and upper limits of control input of the leader are set as $u_{0,min} = -2\ m/s^2$ and $u_{0,max} = 2\ m/s^2$; the weight parameters are set as $\omega_1 = 6$, $\omega_2 = 2$, and $\omega_3 = 1$; the parameters of the band-stop functions are set as $\hat{\alpha} = 2000$, $\hat{\beta} = 2$, $\hat{n} = 1$ and $c = 0.02$.

TABLE 1. Parameters of the vehicle and driveline model.

	m_i(kg)	L_i(m)	μ_i	$A_{i,v}$(m^2)	$C_{i,d}$	$\eta_{i,t}$	τ (s)
Leader	7182	10.0	0.0030	10	0.80	0.940	0.3
Follower 1	7200	11.0	0.0032	10	0.83	0.950	0.3
Follower 2	7100	9.8	0.0031	10	0.81	0.942	0.3
Follower 3	7300	10.5	0.0033	10	0.82	0.938	0.3
Follower 4	7250	10.2	0.0032	10	0.80	0.940	0.3
Follower 5	7310	9.6	0.0031	10	0.81	0.937	0.3

A. INTERNAL STABILITY

According to the sufficient condition of internal stability in ***Theorem*** 1, to achieve the internal stability of vehicle platoon, the control parameters, i.e., α and β, should be properly set to ensure that the upper bound of the input delay is larger than τ in the platoon. When $\alpha = 0.5$ and $\beta = 0.5$, it can be calculated that the upper bound of the input delay is 0.71 s, which is much larger than τ. Therefore, the internal stability of vehicle platoon will be analyzed under $\alpha = 0.5$ and $\beta = 0.5$.

When $\alpha = \beta = 0.5$, the evolutions of spacing errors, velocities and control inputs of vehicles in the platoon can be seen in FIGURE 3, where the initial errors of vehicles in the platoon are not zeros, and the initial velocities of vehicles are different. After the distributed control protocols are applied to the followers, due to different initial spacings and initial velocities, different control inputs are generated for different followers at beginning, hereafter all control inputs gradually decrease to zero over time, see FIGURE 3(c); as time goes on, the velocities of followers reach the same as the leader (i.e., 12 m/s) in FIGURE 3(b); the spacing errors between inter-vehicles converge to 0 m in FIGURE 3(a) when time is about 20 s. These results show, using the proposed

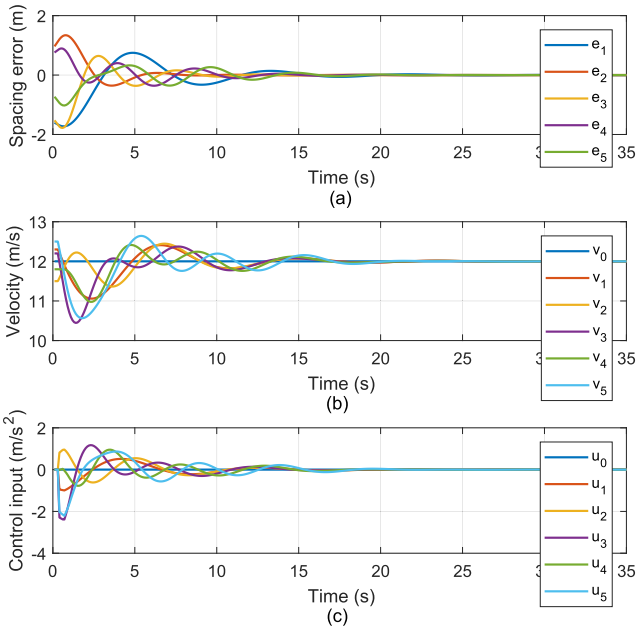

FIGURE 3. The evolutions of positions, spacing errors, velocities and control inputs of vehicles in the platoon when $\alpha = \beta = 0.5$.

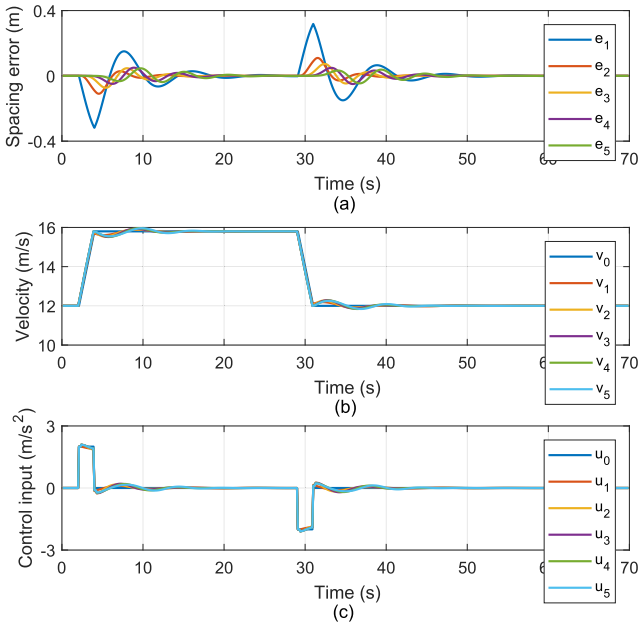

FIGURE 4. The evolutions of spacing errors, velocities and control inputs of vehicles in the platoon when $\alpha = \beta = 0.5$.

distributed protocols, the internal stability of vehicle platoon can be guaranteed when the control parameters are set as $\alpha = \beta = 0.5$.

B. STRING STABILITY

According to the sufficient condition of string stability in ***Theorem*** 2, to achieve the string stability of vehicle platoon, the control parameters, i.e., α and β, should be properly set to ensure that the upper bound of the input delay is larger than τ in the platoon. It can be calculated that, when $\alpha = 0.5$ and $\beta = 0.5$, the upper bound of the input delay is 0.5 s, which is much larger than τ. In addition, the internal stability of vehicle platoon can also be guaranteed when $\alpha = 0.5$ and $\beta = 0.5$. Therefore, the string stability of vehicle platoon will be analyzed under $\alpha = 0.5$ and $\beta = 0.5$.

When $\alpha = \beta = 0.5$, the evolutions of spacing errors, velocities and control inputs of vehicles in the platoon can be seen in FIGURE 4, where the initial errors of followers in the platoon are zeros. In this article, the changes in the acceleration of the leader are regarded as the disturbances on the platoon. And the disturbances are given as

$$a_0(t) = \begin{cases} 2\ \text{m/s}^2, & 2\ \text{s} \le t < 4\ \text{s} \\ -2\ \text{m/s}^2, & 29\ \text{s} \le t < 31\ \text{s} \\ 0, & \text{else} \end{cases} \tag{60}$$

It can be seen in FIGURE 4 that, under the acceleration and deceleration disturbance influences of the leader, the followers also correspondingly accelerate and then decelerate, see FIGURE 4(c); in FIGURE 4(b), when the disturbances disappear, the velocities of followers reach the same as that of the leader after short and small fluctuations; after the disturbances happen, the amplitude of the spacing error e_{i+1} is smaller than that of the spacing error e_i, and all spacing errors return to zero over time, see FIGURE 4(a). These results demonstrate, using the proposed distributed protocols, the string stability of vehicle platoon can be guaranteed when the control parameters are set as $\alpha = \beta = 0.5$.

C. FUEL ECONOMY

After the Eco-CACC strategy is used to control the vehicle platoon, the evolutions of spacing errors, velocities and fuel consumption of vehicles travelling on the simulated highway with varying slopes can be seen in FIGURE 5. In the MPC, the velocity band is set as $[v_l, v_u] = [10, 15]$, and FIGURE 5(b) shows that the velocities fluctuate between 12 m/s and 14 m/s, which are in the velocity band; under the continuous disturbance influences of the leader, the spacing errors of followers are controlled very small, see FIGURE 5(a), and the maximum absolute errors of spacings of follower 1, follower 2, follower 3, follower 4 and follower 5 are 0.0612 m, 0.0218 m, 0.0161 m, 0.0142 m and 0.0134 m, respectively.

To better display the evolutions of spacing errors, the spacing errors from 230 s to 255 s are zoomed in. From the evolutions of spacing errors from 230 s to 255 s, some researchers might make a wrong conclusion that vehicle platoon is not string stable based on the fact that the spacing errors are sometimes amplified upstream. To demonstrate that the string stability defined in (11) is not violated, taking Fast Fourier Transform for the time-domain spacing errors, then the logarithmic amplitude-frequency response from the spacing error of follower $i+1$ to the spacing error of follower i can be seen in FIGURE 6, where $i = 1$ in FIGURE 6(a), $i = 2$ in FIGURE 6(b), $i = 3$ in FIGURE 6(c), and $i = 4$

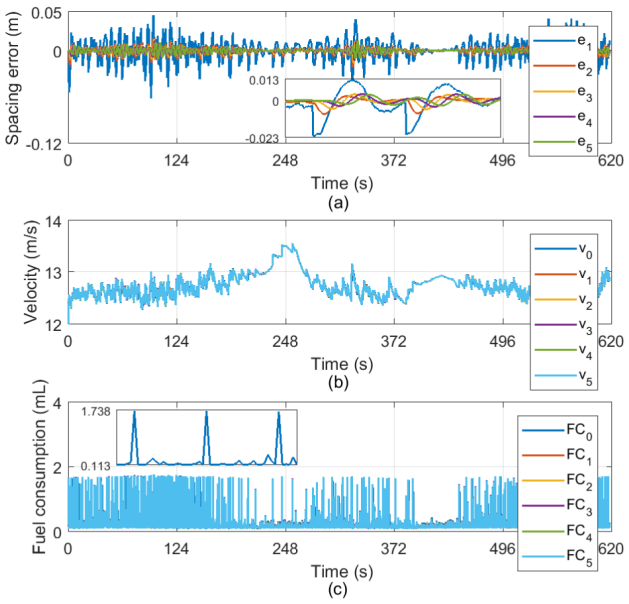

FIGURE 5. The evolutions of spacing errors, velocities and fuel consumption of vehicles travelling on the simulated highway with varying slopes controlled by the proposed Eco-CACC strategy.

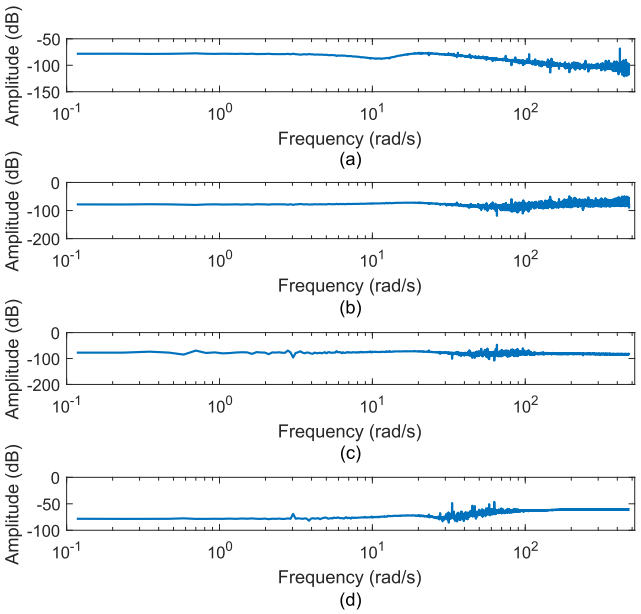

FIGURE 6. The logarithmic amplitude-frequency responses.

in FIGURE 6(d). It can be seen from FIGURE 6, the maximum amplitudes are all much smaller than 1, which demonstrates that the string stability defined in (11) is not violated.

To explain why the velocities in the platoon fluctuate on the simulated highway with varying slopes, the evolution of the leader's fuel consumption from 128 s to 133 s is zoomed in. Considering the idle fuel consumption per time interval is 0.113 mL, the engine of the leader constantly switches between busy operating points and idle operating points, see FIGURE 5(c). If the engine works on the idle operating points, it will consume the least fuel and not output drive power, then, the vehicle will decelerate; otherwise, the engine will consume more fuel and output drive power, then, the vehicle will accelerate. Therefore, the velocities in the platoon fluctuate on the simulated highway. It should be noted that, the passenger comfort might be slightly affected by the fluctuations of velocities, which is the cost of improving the fuel economy due to the nonlinear relationship between fuel consumption rate and engine output power. However, in theory, the fluctuations of velocities can be regulated to be acceptable by properly setting the weights and the allowed range of the control input.

Furthermore, for comparison, the evolutions of spacing errors, velocities and fuel consumption of vehicles travelling on the simulated highway with varying slopes controlled by the benchmark strategy can be seen in FIGURE 7. Since the initial velocities of vehicles are smaller than the reference one, all vehicles accelerate in the beginning. When the velocities of vehicles are the same as the reference one, they will not change any more, see FIGURE 7(b). Before the velocities approach to the reference one, the spacing errors show small and short fluctuations, however, they are not amplified upstream, and converge to zeros over time, see FIGURE 7(a). And the evolutions of the fuel consumption of vehicles in FIGURE 7(c) are not out of our expectation.

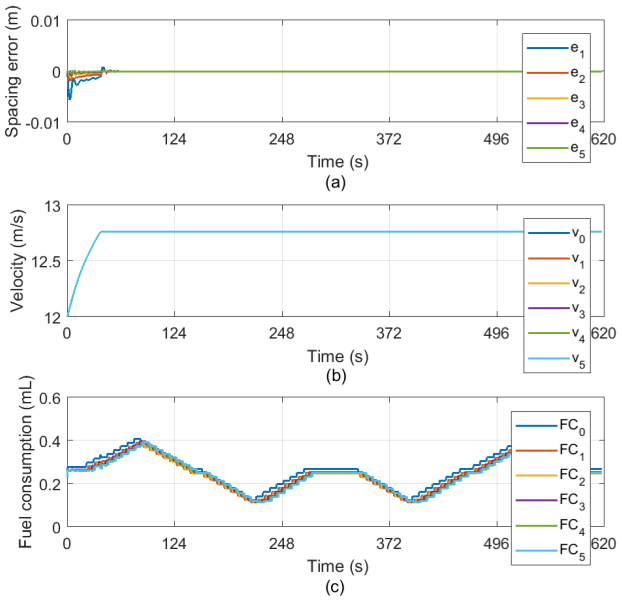

FIGURE 7. The evolutions of spacing errors, velocities and fuel consumption of vehicles travelling on the simulated highway with varying slopes controlled by the benchmark strategy.

To demonstrate the effectiveness of the proposed Eco-CACC strategy on improving the fuel economy of vehicle platoon, the fuel consumption of vehicles on the highway with varying slopes controlled by Eco-CACC and benchmark is given in TABLE 2. As shown in TABLE 2, compared with the benchmark, the fuel consumption of the leader, follower 1, follower 2, follower 3, follower 4 and follower 5

TABLE 2. The fuel consumption (mL) of vehicles on the highway with varying slopes controlled by Eco-CACC and benchmark.

	Leader	Follower 1	Follower 2	Follower 3	Follower 4	Follower 5	Total
Eco-CACC	1540.2	1452.1	1442.5	1458.2	1436.6	1436.0	8765.6
Benchmark	1654.5	1545.6	1528.8	1558.0	1533.6	1539.2	9359.7

is decreased by 6.91%, 6.05%, 5.64%, 6.41%, 6.32% and 6.70%, respectively, and the total fuel consumption of vehicle platoon is reduced by 6.35%. Therefore, compared with the benchmark, the proposed Eco-CACC can significantly reduce the fuel consumption of vehicle platoon.

VI. CONCLUSION

In this article, a highway-based Eco-CACC strategy is proposed for a heterogeneous platoon of heavy-duty vehicles with time delays. The proposed Eco-CACC strategy consists of distributed control protocols for the followers and model predictive controller for the leader. For the platoon of vehicles under PLF communication topology, the sufficient conditions of internal stability and string stability are derived, and the upper bound of the input delay under the given control parameters is also obtained. To further improve the overall fuel economy of vehicle platoon, the control inputs of the leader are optimized by formulating the CIO-LV problem based on MPC. Simulations are conducted to validate the theoretical results, and simulation results show that the proposed Eco-CACC can save 6.35% of fuel for the heterogeneous platoon.

Compared to the second-order differential model, the third-order one has higher accuracy in describing the longitudinal dynamics of heterogeneous vehicles. To achieve better control performance, the distributed control protocols will be designed based on third-order differential model for heterogeneous vehicles in the future. Considering the difference between second-order model and third-order one, the approach applied on the second-order model should be properly modified when being employed to design control protocols based on the third-order one. Furthermore, for safety consideration, the CTH policy is more rational than the CS policy. Hence, we will investigate the CTH policy for the third-order vehicle platoon system with time-varying input delays in the near future.

REFERENCES

[1] G. Guo and Q. Wang, "Fuel-efficient en route speed planning and tracking control of truck platoons," *IEEE Trans. Intell. Transport. Syst.*, vol. 20, no. 8, pp. 3091–3103, Aug. 2019.
[2] Q. Guo, L. Li, and X. Ban, "Urban traffic signal control with connected and automated vehicles: A survey," *Transp. Res. C, Emerg. Technol.*, vol. 101, pp. 313–334, 2019.
[3] K. Liang, J. Mårtensson, and K. H. Johansson, "Heavy-duty vehicle platoon formation for fuel efficiency," *IEEE Trans. Intell. Transport. Syst.*, vol. 17, no. 4, pp. 34–56, Apr. 2016.
[4] D. R. Lopes and S. A. Evangelou, "Energy savings from an eco-cooperative adaptive cruise control: A BEV platoon investigation," in *Proc. 18th Eur. Control Conf. (ECC)*, Jun. 2019, pp. 4160–4167.
[5] C. Zhai, F. Luo, Y. Liu, and Z. Chen, "Ecological cooperative look-ahead control for automated vehicles travelling on freeways with varying slopes," *IEEE Trans. Veh. Technol.*, vol. 68, no. 2, pp. 1208–1221, Feb. 2019.
[6] C. Bonnet and H. Fritz, "Fuel consumption reduction in a platoon: Experimental results with two electronically coupled trucks at close spacing," SAE Tech. Paper 2000-01-3056, Aug. 2000.
[7] F. Browand, J. McArthur, and C. Radovich, "Fuel saving achieved in the field test of two tandem trucks," Calif. Partners Adv. Transit Highways, Berkeley, CA, USA, Tech. Rep. UCB-ITS-PRR-2004-20, Jun. 2004.
[8] J. N. Barkenbus, "Eco-driving: An overlooked climate change initiative," *Energy Policy*, vol. 38, no. 2, pp. 762–769, Feb. 2010.
[9] B. Liu and A. El Kamel, "V2X-based decentralized cooperative adaptive cruise control in the vicinity of intersections," *IEEE Trans. Intell. Transport. Syst.*, vol. 17, no. 3, pp. 644–658, Mar. 2016.
[10] B. HomChaudhuri, A. Vahidi, and P. Pisu, "Fast model predictive control-based fuel efficient control strategy for a group of connected vehicles in urban road conditions," *IEEE Trans. Control Syst. Technol.*, vol. 25, no. 2, pp. 760–767, Mar. 2017.
[11] S. Stebbins, M. Hickman, J. Kim, and H. L. Vu, "Characterising green light optimal speed advisory trajectories for platoon-based optimisation," *Transp. Res. C, Emerg. Technol.*, vol. 82, pp. 43–62, Sep. 2017.
[12] X. He and X. Wu, "Eco-driving advisory strategies for a platoon of mixed gasoline and electric vehicles in a connected vehicle system," *Transp. Res. D, Transp. Environ.*, vol. 63, pp. 907–922, Aug. 2018.
[13] S. E. Li, R. Li, J. Wang, X. Hu, B. Cheng, and K. Li, "Stabilizing periodic control of automated vehicle platoon with minimized fuel consumption," *IEEE Trans. Transport. Electrific.*, vol. 3, no. 1, pp. 259–271, Mar. 2017.
[14] V. Turri, B. Besselink, and K. H. Johansson, "Cooperative look-ahead control for fuel-efficient and safe heavy-duty vehicle platooning," *IEEE Trans. Control Syst. Technol.*, vol. 25, no. 1, pp. 12–28, Jan. 2017.
[15] C. Zhai, Y. Liu, and F. Luo, "A switched control strategy of heterogeneous vehicle platoon for multiple objectives with state constraints," *IEEE Trans. Intell. Transport. Syst.*, vol. 20, no. 5, pp. 1883–1896, May 2019.
[16] A. Alam, B. Besselink, V. Turri, J. Mårtensson, and K. H. Johansson, "Heavy-duty vehicle platooning for sustainable freight transportation: A cooperative method to enhance safety and efficiency," *IEEE Control Syst. Mag.*, vol. 35, no. 6, pp. 34–56, Dec. 2015.
[17] K. Yu, H. Yang, X. Tan, T. Kawabe, Y. Guo, Q. Liang, Z. Fu, and Z. Zheng, "Model predictive control for hybrid electric vehicle platooning using slope information," *IEEE Trans. Intell. Transport. Syst.*, vol. 17, no. 7, pp. 1894–1909, Jul. 2016.
[18] B. Sakhdari and N. L. Azad, "A distributed reference governor approach to ecological cooperative adaptive cruise control," *IEEE Trans. Intell. Transport. Syst.*, vol. 19, no. 5, pp. 1496–1507, May 2018.
[19] C. Zhai, F. Luo, and Y. Liu, "Cooperative look-ahead control of vehicle platoon travelling on a road with varying slopes," *IET Intell. Transp. Syst.*, vol. 13, no. 2, pp. 376–384, Feb. 2019.
[20] C. Zhai, F. Luo, and Y. Liu, "Cooperative look-ahead control of vehicle platoon for maximizing fuel efficiency under system constraints," *IEEE Access*, vol. 6, pp. 37700–37714, 2018.
[21] Y. Zheng, S. E. Li, K. Li, F. Borrelli, and J. K. Hedrick, "Distributed model predictive control for heterogeneous vehicle platoons under unidirectional topologies," *IEEE Trans. Control Syst. Technol.*, vol. 25, no. 3, pp. 899–910, May 2017.
[22] Y. Zheng, S. Li, J. Wang, D. Cao, and K. Li, "Stability and scalability of homogeneous vehicular platoon: Study on the influence of information flow topologies," *IEEE Trans. Intell. Transport. Syst.*, vol. 17, no. 1, pp. 14–25, Jan. 2016.
[23] G. J. L. Naus, R. P. A. Vugts, J. Ploeg, M. J. G. van de Molengraft, and M. Steinbuch, "String-stable CACC design and experimental validation: A frequency-domain approach," *IEEE Trans. Veh. Technol.*, vol. 59, no. 9, pp. 4268–4279, Nov. 2010.
[24] J. Ploeg, N. van de Wouw, and H. Nijmeijer, "Lp string stability of cascaded systems: Application to vehicle platooning," *IEEE Trans. Control Syst. Technol.*, vol. 22, no. 2, pp. 786–793, Mar. 2014.
[25] Y. Liu, H. Gao, C. Zhai, and W. Xie, "Internal stability and string stability of connected vehicle systems with time delays," *IEEE Trans. Intell. Transport. Syst.*, early access, May 24, 2020, doi: 10.1109/TITS.2020.2988401.
[26] H. Chehardoli, "Robust optimal control and identification of adaptive cruise control systems in the presence of time delay and parameter uncertainties," *J. Vibrat. Control*, Jan. 2020, Art. no. 1077546319901086, doi: 10.1177/1077546319901086.
[27] H. Chehardoli, A. Ghasemi, and A. Najafi, "Centralized and decentralized distributed control of longitudinal vehicular platoons with non-uniform communication topology," *Asian J. Control*, vol. 21, no. 6, pp. 2691–2699, Nov. 2020.

[28] W. H. Hucho, *Aerodynamics Road Vehicles*. London, U.K.: Butterworth, 1987.
[29] J. Wang and H. A. Rakha, "Fuel consumption model for heavy duty diesel trucks: Model development and testing," *Transp. Res. D, Transp. Environ.*, vol. 55, pp. 127–141, Aug. 2017.
[30] K. Santhanakrishnan and R. Rajamani, "On spacing policies for highway vehicle automation," *IEEE Trans. Intell. Transport. Syst.*, vol. 4, no. 4, pp. 198–204, Dec. 2003.
[31] M. Pirani, E. Hashemi, J. W. Simpson-Porco, B. Fidan, and A. Khajepour, "Graph theoretic approach to the robustness of k-nearest neighbor vehicle platoons," *IEEE Trans. Intell. Transport. Syst.*, vol. 18, no. 11, pp. 198–204, Nov. 2017.
[32] H. Chehardoli and A. Ghasemi, "Adaptive centralized/decentralized control and identification of 1-d heterogeneous vehicular platoons based on constant time headway policy," *IEEE Trans. Intell. Transport. Syst.*, vol. 19, no. 10, pp. 3376–3385, Oct. 2018.
[33] Y. A. Harfouch, S. Yuan, and S. Baldi, "An adaptive switched control approach to heterogeneous platooning with intervehicle communication losses," *IEEE Trans. Control Netw. Syst.*, vol. 5, no. 3, pp. 1434–1444, Sep. 2018.
[34] S. Baldi, D. Liu, V. Jain, and W. Yu, "Establishing platoons of bidirectional cooperative vehicles with engine limits and uncertain dynamics," *IEEE Trans. Intell. Transport. Syst.*, early access, Feb. 24, 2020, doi: 10.1109/TITS.2020.2973799.
[35] Y. Liu, B. Xu, and Y. Ding, "Convergence analysis of cooperative braking control for interconnected vehicle systems," *IEEE Trans. Intell. Transport. Syst.*, vol. 18, no. 7, pp. 1894–1906, Jul. 2017.
[36] P. Seiler, A. Pant, and K. Hedrick, "Disturbance propagation in vehicle strings," *IEEE Trans. Autom. Control*, vol. 49, no. 10, pp. 1835–1841, Oct. 2004.
[37] S. Oncu, J. Ploeg, N. van de Wouw, and H. Nijmeijer, "Cooperative adaptive cruise control: Network-aware analysis of string stability," *IEEE Trans. Intell. Transport. Syst.*, vol. 15, no. 4, pp. 1527–1537, Aug. 2014.

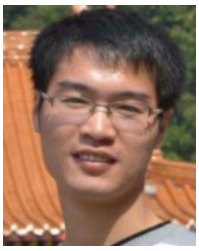

CHUNJIE ZHAI (Member, IEEE) was born in Bozhou, Anhui, China. He received the B.S. degree from the Jiangxi University of Science and Technology, Ganzhou, China, in 2012, and the Ph.D. degree from the South China University of Technology, Guangzhou, China, in 2019. He is currently a Lecturer with the School of Automation, Hangzhou Dianzi University, Hangzhou, China. His main research interests include autonomous vehicle control, cooperative control, and intelligent transportation systems.

XIYAN CHEN was born in Wenzhou, Zhejiang, China. She is currently pursuing the B.S. degree with Hangzhou Dianzi University, Hangzhou, China. Her main research interests include autonomous vehicle control and cooperative control.

CHENGGANG YAN received the B.S. degree in computer science from Shandong University, Jinan, China, in 2008, and the Ph.D. degree in computer science from the Institute of Computing Technology, Chinese Academy of Sciences, Beijing, China, in 2013. He was an Assistant Research Fellow with Tsinghua University. He is currently a Professor with Hanzhou Dianzi Univeristy, Hangzhou, China. His research interests include machine learning, image processing, computational biology, and computational photography. He has authored or coauthored more than 30 refereed journal and conference papers. As a coauthor, he received the Best Paper Awards in the International Conference on Game Theory for Networks, in 2014, and the SPIE/COS Photonics Asia Conference 9273, in 2014; and the Best Paper Candidate in the International Conference on Multimedia and Expo, in 2011.

YONGGUI LIU (Member, IEEE) was born in Hunan, China. He received the B.S. degree in electronic information engineering from the Hunan University of Technology, Zhuzhou, China, in 2001, and the M.S. and Ph.D. degrees from the South China University of Technology, Guangzhou, China, in 2008 and 2011, respectively. He is currently an Associate Professor with the School of Automation Science and Engineering, South China University of Technology. He is also a Postdoctoral Fellow with the Shenzhen Research Institute, The Chinese University of Hong Kong, Shenzhen, China. His main research interests include autonomous vehicle control, cooperative control, networked control systems, wireless sensor/actuator networks, and estimation theory and application.

HUAJUN LI received the B.S. degree in automation from Zhejiang University, in 2012, and the Ph.D. degree from the College of Control Science and Engineering, Zhejiang University, in 2018. He is currently a Lecturer with the School of Automation, Hangzhou Dianzi University. His research interests include intelligent detection and control, optical tomography, and machine learning.